ACS OMEGA

Open Access

This article is licensed under CC-BY-NC-ND 4.0

http://pubs.acs.org/journal/acsodf

Article

Dynamic Detection of the E3-PROTAC-Target Protein Ternary Complex *In Vitro* and *In Vivo via* Bimolecular Fluorescence Complementation

Kunjian Lei, Yilei Sheng, Yishuang Li, Zhihong Zhou, Xingen Zhu,* and Kai Huang*

Cite This: *ACS Omega* 2024, 9, 49739−49748

Read Online

ACCESS | Metrics & More | Article Recommendations | Supporting Information

ABSTRACT: Proteolysis-targeting chimeras (PROTACs) have played an important role in the development of protein-targeted degradation drugs. However, effective tools are urgently required for the further development and validation of PROTACs. We developed a high-potency reporter (AKT-PROTAC-Reporter; APR) for PROTACs that specifically targets AKT. The APR successfully detected the status and levels of the AKT-PROTAC-CRBN ternary complex *in vivo* and *in vitro*. The APR is based on a bimolecular fluorescence complementation system, where EGFP and luciferase were used as reporter signals for *in vitro* and *in vivo* experiments, respectively, with remarkable success. The absence of E3 ligase ubiquitin recruitment activity in the APR can significantly improve the reporting performance of the APR; however, this results in difficulties in the detection of the degradation efficiency of PROTAC target proteins. Our results show that the APR can sensitively, quickly, and effectively detect the presence of terpolymers. Furthermore, the APR can determine the specificity and degradation efficiency of the PROTAC *via* a fluorescence signal or bioluminescence signal intensity and can efficiently screen PROTACs for a certain target protein.

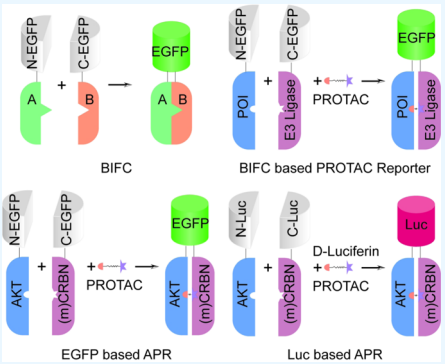

1. INTRODUCTION

In the early 21st century, targeted protein degradation (TPD) was identified as a potential clinical treatment strategy for disease.[1,2] With further development breakthroughs, the outstanding application prospects and transformation potential of TPD have been highlighted.[1,3] Common targets for the degradation of damaged proteins or organelles in eukaryotic cells are the ubiquitin-proteasome system (UPS) and lysosomes.[4,5] Specific target proteins, induced by the UPS for ubiquitination and subsequent degradation, have become the focus of biomedical research. Generally, in the ubiquitination pathway, ubiquitin binds to the target protein *via* the E1/E2/E3 enzyme.[6,7] The function of E3 ligase includes specific recognition of the substrate; thus, small molecule drugs that have been developed based on the UPS-based TPD strategy mainly select E3 ligase as the target protein for degradation.[8] Such drugs include proteolysis-targeting chimeras (PROTACs), molecular glue, and PROTAC-based technologies, including transcription factor (TF)-PROTACs, hydrophobic tagging (HyT), selective androgen receptor degraders (SARDs), selective estrogen receptor degraders (SERDs), and dual-PROTACs.[1,9−12]

The PROTAC molecule consists of a protein of interest (POI) targeting warhead, an E3 recruiting ligand, and a flexible linker connecting the aforementioned elements.[13] The addition of the PROTAC promotes recognition and binding between the POI and E3, which is marked by the formation of the POI-PROTAC-E3 ternary complex, and induces the ubiquitination and subsequent degradation of the POI.[13] In principle, the UPS can degrade any protein that can be recognized by a specific E3 ligase. In most cases, the clinical transformation of PROTACs is difficult in humans; however, by continuing to optimize the components and pharmacokinetic performance of PROTACs, we can further promote the vigorous development of PROTACs.[1] Compared with traditional small molecule inhibitors, PROTACs show many prominent advantages.[14] First, more than 4,000 disease-related proteins have been identified, and PROTAC technology has greatly expanded the range of drug-capable proteins. Second, the POI can be rapidly and effectively targeted by PROTACs, which significantly inhibits the intracellular and extracellular functions of the POI. Importantly, PROTACs are not prone to drug resistance, and can achieve very high clinical benefits and few toxic side effects at low concentrations.

Protein−protein interactions (PPIs), as a fundamental mechanism for generating biological regulatory specificity, are also the basis for the function of PROTACs.[15] Bimolecular

Received: September 5, 2024
Revised: November 19, 2024
Accepted: November 22, 2024
Published: December 3, 2024

© 2024 The Authors. Published by American Chemical Society

fluorescence complementation (BiFC) technology, which is based on the association between two nonfluorescent fragments of a fluorescent protein when they come close to each other through interactions between proteins fused to the fragment, enables the direct visualization of PPIs in living cells.[16] The visualization capabilities based on BiFC analysis have enabled many PPIs to be increasingly revealed in different cell types and organisms.[16] The BiFC system based on EGFP and luciferase has been widely used and has achieved excellent results;[17−21] therefore, our research has flexibly modified the technique to enable visual screening and efficiency verification of PROTACs.

Although PROTACs have great application and exploration value, the selection of E3-recruiting ligands and POI targeting warheads remains extremely challenging. Complex and expensive screening measures are required to screen out accurate and effective PROTACs, and the blood−brain barrier (BBB) hinders the development of drugs for intracranial diseases.[22,23] Therefore, a tool that can quickly visualize whether PROTACs can cross the BBB will undoubtedly be of great help in drug development.

Our study has developed a PROTAC reporter based on BiFC technology and the UPS system. The reporter can accurately and efficiently visualize the status of PROTACs *in vivo* and *in vitro*. These reporters will greatly facilitate the expansion of efficient and usable PROTACs.

2. MATERIALS AND METHODS

2.1. Materials. Two human cell lines cultured in our study, U251 MG and HEK-293T, were acquired from American Type Culture Collection (ATCC). PROTACs targeting AKT1 degradation (MS170, MS5033, MS98, and INY-03-041) were acquired from MedChemExpress (MCE). The proteasome inhibitor MG132 MK2206, Lenalidomide, and dimethyl sulfoxide (DMSO) were acquired from MedChemExpress (MCE). Anti-His, anti-HA, anti-GAPDH, anti-AKT1, anti-Ki67, goat antimouse, and goat antirabbit antibodies were purchased from Proteintech (Wuhan, China). The Plasmid Point Mutation kit and high-fidelity DNA polymerase were obtained from Vazyme (Nanjing, China).

2.2. Construction of Plasmid and Mutagenesis. The pCDH-puro-myr-HA-Akt1, which we used as an overexpression vector, was a gift from Jialiang Wang (Addgene plasmid #46969). After digestion of the vector with XbaI and *Eco*RI enzymes, the nucleotide sequences of the His tag, P2A, and HA tag were first synthesized on the treated vector by Sangon Biotech (Shanghai, China). After the total RNA of glioma cells was reverse-transcribed into cDNA using a total RNA extraction kit (Vazyme, China), fragments of AKT and CRBN were amplified using PCR, and then inserted into the above-mentioned vectors amplified by linearized primers, respectively. Similarly, the PCR-amplified EGFP and luciferase fragments, which were a gift from Thomas Weber (Addgene plasmid #163523), were divided into two segments by primes and then inserted into the aforementioned vector. According to the manufacturer's instructions, the single point mutation kit (Vazyme, China) was used to mutate CRBN (E377 V and V388 I). All primers were synthesized with the help of GENEWIZ (Suzhou, China).

2.3. Cell Culture, Transfection, and Treatment. U251 and 293T cells were cultured in Dulbecco Modified Eagle's Medium (DMEM) supplemented with 10% fetal bovine serum (Gibco) and 1% penicillin and streptomycin (Gibco). Once the cell confluence reached 80%, the cells were transfected with Lipofectamine 3000 transfection reagent (Thermo Fisher Scientific) and cultured for 24−48 h for follow-up treatment. DMSO and MS170 were added to the cell culture medium 12 h after transfection, and subsequent experiments could be performed after the treatment time reached 24 h.

2.4. Western Blotting (WB). Immunoblotting was performed as described previously.[24] Briefly, U251 and 293T cells were lysed in WB lysis buffer (Solarbio, China) with protease inhibitors. The desaturated proteins were loaded into 10% sodium dodecyl-sulfate polyacrylamide gel electrophoresis (SDS-PAGE) gels (25 μg) to separate the protein lysates. Proteins were then transferred to polyvinylidene difluoride (PVDF) membranes, and then probed with the relevant primary antibody, including GAPDH (1:2000, Cell Signaling Technology, CST), His tag (1:2000, Proteintech), HA tag (1:5000, Proteintech), and tubulin (1:2000, Proteintech). Membranes where then incubated in the appropriate HRP-conjugated secondary antibody (1:2000, Proteintech). An imaging system (Tanon, China) was used to visualize target protein bands on the membrane and the results were quantified by ImageJ software.

2.5. Flow Cytometry. Treated cells were collected by centrifugation and resuspended at a concentration of 1×10^6 in phosphate buffered saline (PBS) or DMEM. The green fluorescence level (EGFP) of the cells was then immediately assessed by flow cytometry in the FITC channel. FlowJo was utilized to analyze the flow cytometry experimental data.

2.6. Cell Imaging and Bioluminescent Imaging. Following cell treatment, the green fluorescence intensity (EGFP) and bright field of the cells were captured using the fluorescence microscope (20×, Leica). For cell bioluminescence imaging, luciferin potassium salt (Macklin, China) was dissolved in DMEM and diluted to a working concentration, which was then added to the cell culture plate and incubated for 5−10 min. The cell culture plate was then immediately placed in the luminescence imaging system to detect the luminescence level.

For *in vivo* imaging of mice, an intrabitoneal injection was performed according to the weight of the nude mice (20 g, 100 μL of fluorescein potassium salt). After 10−20 min under isoflurane gas anesthesia, the bioluminescence intensity of the intracranial was monitored by the luminescent imaging system (PerkinElmer). All the acquired bioluminescence data was analyzed with the help of the imaging system's own processing software.

2.7. Construction of Mouse Tumor Models. All animal experiments were approved by the Animal Protection and Use Committee of Nanchang University. Mice were randomly assigned to six experimental groups. Investigators were not blinded to the experiments. Healthy nude mice (Gempharmatech, China), raised in specific pathogen free housing, were used to construct intracranial glioma models at 4 weeks of age. The whole operation was performed under isoflurane anesthesia. The injection point (2.5 mm on the right, 1 mm in front of the halogen) was determined, and 10^5 U251 cells with stable expression of APR or luciferase were injected into each nude mouse. After the injection, the incision was sutured, and the mice were placed back into the cage after 30 min of observation. The growth of the nude mice was recorded. Intrathecal injection of DMSO or MS170 was performed every 4 days until 8 weeks of age. At the end of the experiment, the mice were killed humanely, and the tumor tissue was

https://doi.org/10.1021/acsomega.4c08186
ACS Omega 2024, 9, 49739−49748

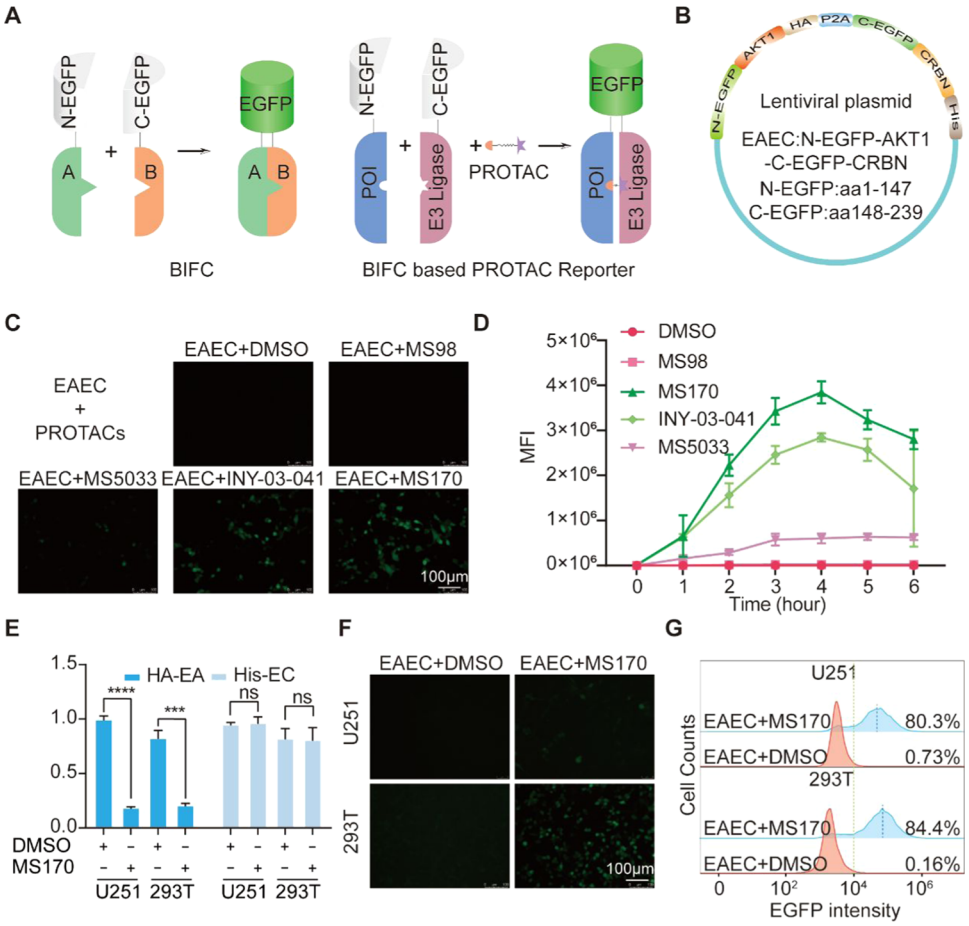

Figure 1. Validation of the AKT-PROTAC-Reporter (APR) in U251 and 293T cells. (A) Left, the working principle of bimolecular fluorescence complementation (BiFC) technology based on EGFP; Right, a working diagram of a reporter dependent on PROTAC's EGFP-based BiFC. (B) Schematic diagram of the plasmid NEGFP-AKT1-P2A-CEGFP-CRBN (EAEC). (C) HEK 293T cells with stable EAEC expression were treated with DMSO, MS1710 (1 μM), MS98 (2 μM), MS5033 (2 μM), or INY-03-041 (200 nM) for 12 h, and the intracellular green fluorescence was captured by fluorescence microscopy (20×). (D) The mean fluorescence intensity (MFI) at different time points after different PROTACs were used to treat U251 cells stably expressing EAEC. (E) The effects of DMSO and MS170 on stable overexpression of HA-EA and His-EC in U251 and 293T cells were studied. The protein immunoblotting results were representative of three independent replicates. After treatment with MS170, HA-EA could be significantly degraded, while His-EC showed no significant difference compared with control group. (F) Fluorescence microscopy (20×) was used to capture the change in the green fluorescence intensity of U251 and 293T cells with stable APR overexpression after treatment with DMSO and MS170 (1 μM) for 12 h. MS170 enables the APR to show microscopically captured green fluorescence inside cells. (G) U251 and 293T cells were digested and suspended, and then flow cytometry was used to further detect the change in the green fluorescence level after MS170 treatment. The proportion of fluorescent cells quantified in this experiment was based on the FITC channel signal intensity of 1×10^4. ****: $p < 0.0001$, ***: $p < 0.001$, ns: not significant. Scale bars = 100 μm.

harvested, fixed with paraformaldehyde, and temporarily preserved.

2.8. Histological Staining. Mice brain tissues were fixed and prepared for staining. Mayer's hematoxylin and eosin (HE) were used sequentially to stain the specimens, which were then mounted on universal slides. Paraffin-embedded mouse brain tissue sections were stained with Ki67.

2.9. Statistical Analyses. The two-tailed *t* test was utilized to assess the differences between different experimental groups. The Kaplan−Meier model and bilateral log-rank test were used to analyze the survival of nude mice. The results of the statistical significance tests are included in the legend for each graph. Where possible, the results were confirmed in multiple independently replicated experiments. ****: $p < 0.0001$, ***: $p < 0.001$, **: $p < 0.01$, *: $p < 0.05$, ns: not significant. Most of the experimental conclusions are derived from the results of three independent replications. $p < 0.05$ was considered statistically significant.

3. RESULTS

3.1. PROTAC Reporter: The E3-PROTAC-POI Ternary Complex Could Be Detected with the BiFC System Based on EGFP. Recently, PROTACs have attracted increasing attention, and have been reported to have the following advantages over most small molecule inhibitors:[14] (1) PROTACs greatly expand the range of proteins that can be targeted for degradation. (2) They are able to overcome the limitations of drug resistance and prolong the drug action time. (3) They have a high degradation activity and excellent safety profile with only a small dose. (4) There is higher selectivity in some targets of the POI. Therefore, PROTACs are considered as a revolutionary technology. However, we should also note some of the limitations of PROTACs, such as an excessive relative molecular weight, dependence on specific E3 ligases, and so on.[25] To design a reporter that can quickly show whether a PROTAC is working, we first developed a PROTAC reporter (PR) based on the BiFC system. The mechanism of

https://doi.org/10.1021/acsomega.4c08186
ACS Omega 2024, 9, 49739−49748

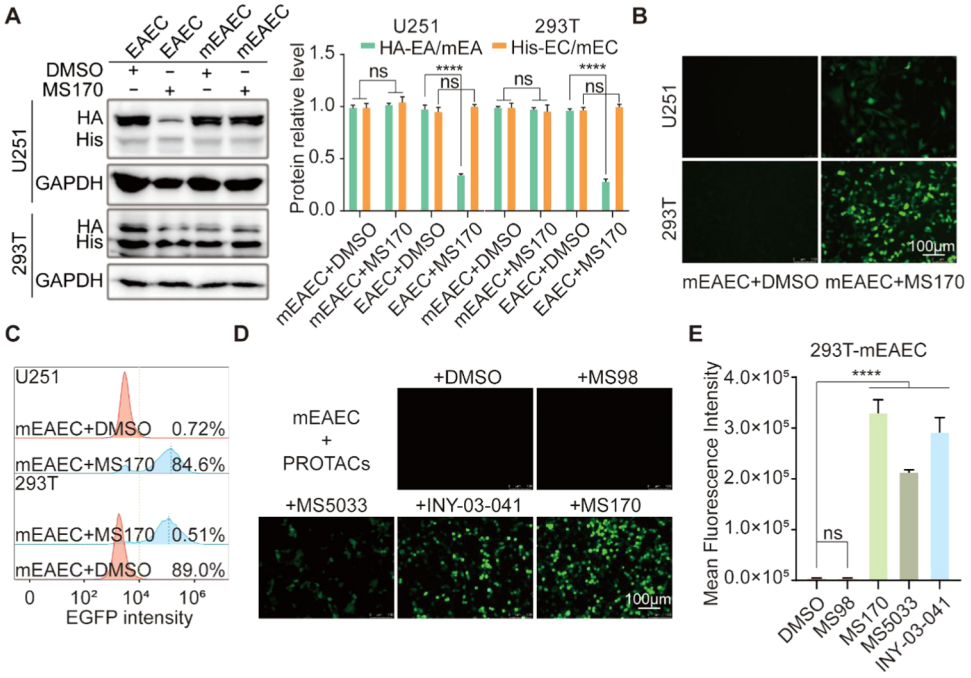

Figure 2. AKT-PROTAC-Reporter (APR) still has reporter performance after CRBN mutation. (A) After DMSO or MS170 was added to U251 and 293T cells, the levels of HA-EA/mEA and His-EC/mEC were detected by immunoblotting, and GAPDH was used as the internal reference. (B) The U251 and 293T cells that stabilized the mutated APR were treated with DMSO or MS170 and their fluorescence was observed by fluorescence microscopy (20×). (C) U251 or 293T cells was suspended and flow cytometry was used to further detect the change in the green fluorescence level after MS170 treatment. The quantitative fluorescence cell ratio in this experiment was based on the signal intensity of the FITC channel of 1×10^4. The 293T cells stably expressing mEAEC were treated with DMSO, MS1710, MS98, MS5033, or INY-03-041 for 12 h, photographed using fluorescence microscopy (20×) (D); FITC channel signals were detected by flow cytometry and the average fluorescence intensity (E) was calculated ****: $p < 0.0001$, ns: not significant. Scale bars = 100 μm.

the PR is shown in Figures 1A and S1A. The two nonfluorescent fragments formed by the disconnection of EGFP at site 149 can emit green fluorescence after getting close to each other.[26] Theoretically, the PR mainly reflects the ability and state of PROTACs to combine with the POI and E3 ligase to form ternary complexes, which is specifically manifested as nonfluorescent fragments that get close to each other and emit green fluorescence.

The expression level of AKT is increased or overactivated in a variety of human primary solid tumors.[27,28] Primary glioma is the most common intracranial primary tumor in adults, and the increase or abnormal activation of AKT at the protein level is generally observed in tumor cells. Therefore, use of a PR targeting AKT is of great significance for glioma and other tumors affected by AKT carcinogenesis. Our study first examined the performance of several PROTACs targeting AKT and CRBN (MS170, MS5033, and INY-03-041) and one PROTAC targeting AKT and pVHL (MS98).[29−31]

To obtain stable and efficient expression of the AKT-PROTAC-Reporter (APR) in 293T cells, we first constructed the NEGFP-AKT1-CEGFP-CRBN (EAEC) plasmid (Figure 1B). Cells stably overexpressing EAEC were treated with DMSO, MS170, MS5033, MS98, and INY-03-041. With MS98 treatment, the two nonfluorescent fragments of EGFP were separated and could not display green fluorescence because MS98 could not bind specifically to CRBN. MS170, MS5033, and INY-03-041 resulted in the normal function of the APR, among which MS170 shown a stronger degradation efficiency and binding ability. These conclusions were based on a combination of captured fluorescence images, FITC channel signal detection by flow cytometry, and protein level detection by EAEC (Figures 1B−D, and S1B−D); therefore, we selected MS170 for follow-up analysis. Furthermore, it was determined that the APR could specifically report the performance of the appropriate PROTAC. Considering that the position of the POI and E3 ligase in recombinant proteins may affect binding to MS170, we also constructed three different combinations of fusion proteins to detect the function of APR (Figure S1E). With the help of the overexpression system, we achieved the expression of multiple fusion proteins in 293T cells. After MS170 was added into the culture system, only EAEC showed a significant green fluorescence signal (Figure S1F). Although AECE was also positive, it was obvious that EAEC had the best display performance as an APR. Meanwhile, flow cytometry further identified the potential of EAEC as an APR by monitoring FITC channel signals in 293T cells that expressed different fusion proteins after MS170 treatment (Figure S1G). Although the effect of MS170 could be visualized by the APR, it was necessary to confirm that the E3-PROTAC-target protein ternary complex was degraded by the ubiquitination pathway. Therefore, we added an additional proteasome inhibitor, MG132, to block intracellular protein degradation *via* the ubiquitination pathway. The results show that adding MG132 at 4 h after treating cells with MS170 can significantly inhibit the decrease in cell fluorescence intensity (Figure S1H). In addition, we also detected the expression levels of various fusion proteins in 293T cells. In the EAEC group, MS170 could only significantly reduce the levels of HA-EA and endogenous ones, but had no effect on the levels of His-EC (Figure S2A,B). More importantly, we also dynamically monitored the performance of various APRs in the presence

https://doi.org/10.1021/acsomega.4c08186
ACS Omega 2024, 9, 49739−49748

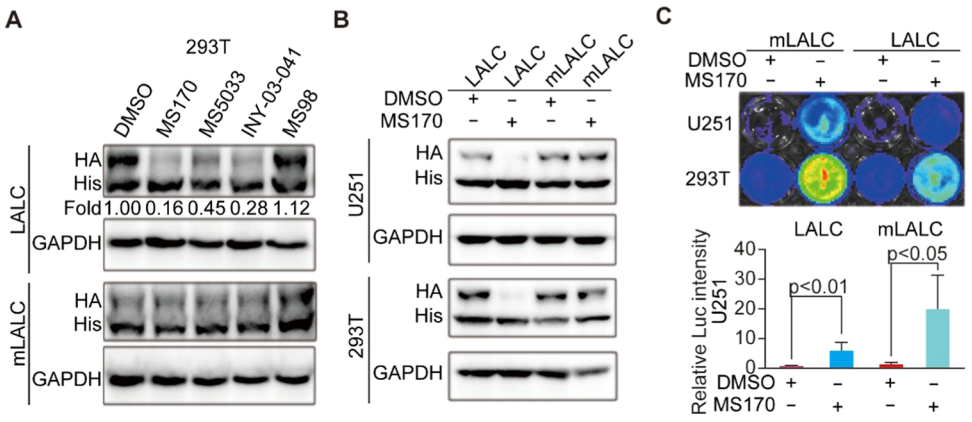

Figure 3. Validation of the application of the luciferase-based AKT-PROTAC-Reporter (APR) in cells. (A) DMSO, MS1710, MS98, MS5033, or INY-03-041 treatment of 293T or U251 cells that stably expressed LALC for 24 h. Protein imprinting was performed to detect the protein levels of LA and LC. (B) After the U251 and 293T cells stabilized the mutated APR, the DMSO or MS170 levels of HA-LA and His LC were detected by Western blotting. (C) Upper, U251 and 293T cells statically overexpressing LALC or mLALC were treated with DMSO or MS170 and the total fluorescence signal level was detected using a bioluminescent imaging system. Bottom, the fluorescence signals detected in U251 cells were quantified for statistical analysis, and $p < 0.05$ was considered statistically significant.

of MS170, which fully confirmed the reliability of EAEC and the dynamic response ability of the reporter (Figure S2C,D).

To further determine the application potential of EAEC in human tumor cells, we stably expressed EAEC in HEK 293T and glioma U251 cells. After treatment with MS170, the HA-EA level in the cells was significantly reduced and the green fluorescence was significantly enhanced (Figure 1E,1F). Further verification was performed by flow cytometry (Figure 1G). In addition, we further determined whether MG132, AKT1 ligand or CRBN ligand would affect the formation of the ternary complex or the intensity of the fluorescence signal. Therefore, we added DMSO, MG132, MK2206 or Lenalidomide after treating the cells with MS170. The results showed that MG132 could stabilize the fluorescence signal, while MK2206 or Lenalidomide would compete with MS170 for binding to AKT1 or CRBN, thereby significantly inhibiting the reporting performance of EAEC (Figure S3A−D). These conclusions indicate that EAEC can reliably report the effects of MS170 on AKT1, and that the reporting performance of EAEC is dependent on the proteasome pathway.

3.2. Mutated E3 Significantly Enhanced the Performance of the PR. In a previous study, we found that MS170 significantly reduced the intracellular level of EAEC, even though it resulted in the formation of green fluorescence that could be captured by fluorescence microscopy; however, this is not conducive to an improvement in the visualization efficiency. The decrease in HA-EA is mainly due to the ubiquitination degradation of HA-EA after the formation of the ternary complex between APR and MS170, which weakens the visualization efficiency of APR to some extent. Therefore, to obtain a more stable and reliable APR, eliminating its ability to recruit E2 while preserving its ability to bind to MS170, we constructed a mutant EAEC (mEAEC: E377 V and V388I) (Figure S4A).[32,33] Next, we verified the expression of EAEC and mEAEC in 293T and U251 cells using an overexpression system. As shown in Figure 2A, the expression of EAEC and mEAEC was detected in both 293T and U251 cells, but the presence of MS170 did not significantly reduce the protein level of HA-EA in the mEAEC group, which is in sharp contrast to the significant reduction shown with EAEC. To determine whether the mEAEC can also show the status of the ternary complex, we added MS170 to 293T and U251 cells with stable expression of EAEC or mEAEC, and found that the mEAEC group had a higher green fluorescence intensity than the EAEC group (Figure 2B). Furthermore, flow cytometry also showed the excellent reporting performance of the mEAEC (Figure 2C). To determine whether the mEAEC could be applied to other PROTACs, 293T cells were treated with MS98, MS5033, and INY-03-041. As expected, the PROTACs failed to reduce the level of HA-EA, MS98 failed to result in an mEAEC-mediated green fluorescence signal that could be captured, and MS5033 and INY-03-041 reacted with mEAEC in 293T cells to generate a lower green fluorescence intensity than MS170, although significantly better than EAEC (Figures 2D,E, and S4B). These results show that mEAEC as an APR has better visualization performance than EAEC.

3.3. Luciferase Was Also Suitable for Constructing the APR. The EGFP-based APR showed a good performance *in vitro*, but its weak tissue penetration and low signal-to-noise ratio make it difficult to flexibly apply to *in vivo* studies compared with luciferase.[34,35] To further extend the application of the APR to *in vivo* experiments, we replaced the EGFP with luciferase to achieve the following functions: (1) an absent or weak bioluminescence signal when the PROTAC is not present; (2) a significant bioluminescence signal after adding the PROTAC; and (3) can be used for *in vivo* mouse imaging. Studies have shown that when luciferase splits into two parts ($NLuc^{1-416}$ and $C\text{-}Luc^{398-550}$), they lose enzymatic activity, but as they move closer to each other, they regain enzymatic activity.[36] Therefore, we designed APRs for *in vivo* experiments as follows: NLuc-AKT-P2A-CLuc-CRBN (LALC) and NLuc-AKT-P2A-CLuc-mCRBN (mLALC) (Figure S4C).

Similarly, we first examined the expression levels of LALC and mLALC in 293T and U251 cells and obtained results consistent with expectations; only appropriate PROTACs were able to make the LALC work (Figures 3A and S4D). MS170 could significantly reduce the expression level of HA-LA in the LALC group, which could be blocked by MG132 (Figure S4E), while the mLALC group was not significantly affected (Figure 3B). In addition, MG132 could effectively reverse the decrease in the HA-LA expression level in the LALC group (Figure S2C). To further determine the visualization potential of luciferase-based APRs, we performed bioluminescence

https://doi.org/10.1021/acsomega.4c08186
ACS Omega 2024, 9, 49739−49748

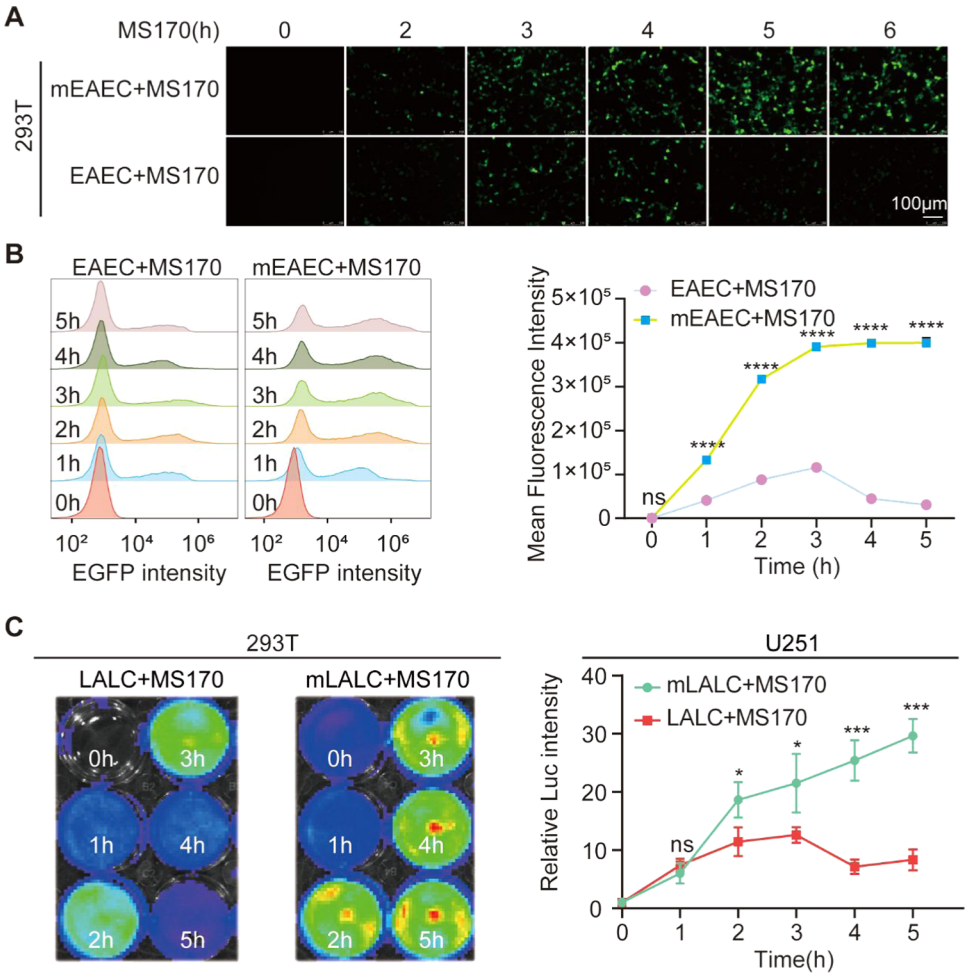

Figure 4. AKT-PROTAC-Reporter (APR) showed the time-dependent effect of the PROTAC *in vitro*. (A) U251 and 293T cells expressing EAEC or mEAEC were treated with MS170, respectively, and green fluorescence changes with time were observed by fluorescence microscope (20×). (B) After MS170 treatment, FITC channel signals of 293T cells were detected at different time points. Left, mEAEC or EAEC were used to detect EGFP levels over time by flow cytometry after MS170 treatment. Right, the intracellular mean fluorescence intensity (MFI) at different time points after MS170 treatment. (C) Left, using an imaging system to detect images of the 293T cells in the MS170 treated pore plate at different time points of action. Right, the line chart shows the change of fluorescence signal in U251 cells over time and the difference in the fluorescence signal between LALC and mLALC at the same time point. ***: $p < 0.001$, **: $p < 0.01$, *: $p < 0.05$, ns: not significant. Scale bars = 100 μm.

imaging using 293T and U251 cells that stably express LALC and mLALC. Although the LALC group exhibited some bioluminescence intensity in the presence of MS170 (Figure 3C), it was obvious that mLALC is more suitable as an APR. These results suggest that mLALC may be a promising APR for *in vivo* studies.

3.4. PR Can Indicate the Appropriate Concentration and Duration of Action of the PROTAC Drug. To further characterize the reporter features of the APR, we first recorded the green fluorescence levels at different time points after treating stable EAEC- and mEAEC-expressing 293T cells with MS170 or DMSO. MS170 was effective quickly and the APR response was sensitive, reaching a peak at around 2 h, which was consistent with our expectations. The fluorescence level of EAEC decreased as the ternary complex degraded, while the fluorescence level of the mEAEC group could be maintained at a relatively high level (Figure 4A,B). It is worth noting that we also detected the APR protein levels at different time points after treating 293T and U251 cells with MS170, and the results were consistent with the flow cytometry results, with mEAEC maintaining a stable protein level (Figure S3A,B). This indicates that the APR exhibits time-dependent characteristics with the PROTAC and shows different fluorescence levels over time, with the mLALC reporting excellent stability.

The two APRs showed significant differences in bioluminescent levels, with mLALC achieving a peak bioluminescent level at 2 h and maintaining a high level of bioluminescent intensity for 6 h, a finding that was consistent in both 293T and U251 cells (Figure 4C). In both 293T and U251 cells, MS170 treatment resulted in a drastic decrease in LALC protein levels, reflecting significant reporter activity attenuation. However, mLALC was able to overcome this drawback and maintain good PR activity for at least 6 h. Therefore, mLALC will be used as the appropriate APR for subsequent *in vivo* studies.

3.5. Luciferase-Based PR Shows the Effects of PROTAC Drugs *In Vivo*. Following *in vitro* validation of PROTACs, they often require numerous studies *in vivo* to determine their target protein degradation profile, and the binding efficiency of PROTAC combined with E3 ligase and the target protein cannot be visualized. Thus, we designed APRs to intuitively display the status of the E3-PROTAC-POI. As the luminescence intensity of the APR is often correlated with the ternary complex content, the APR can effectively

https://doi.org/10.1021/acsomega.4c08186
ACS Omega 2024, 9, 49739−49748

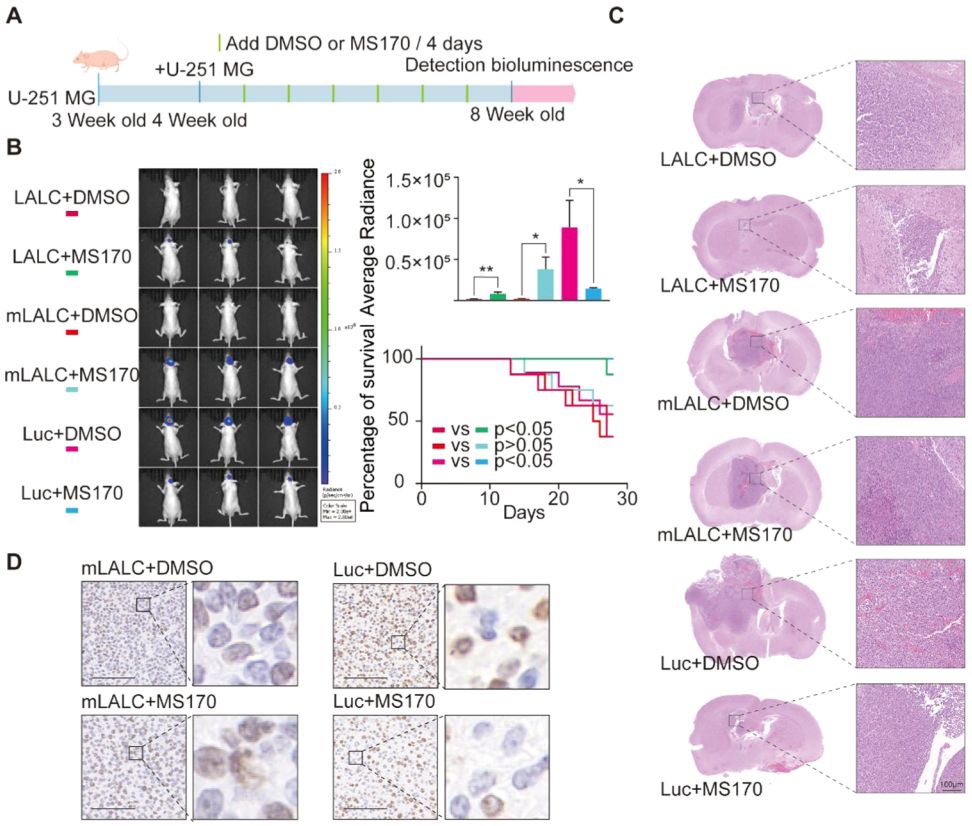

Figure 5. Validation of the AKT-PROTAC-Reporter (APR) *in vivo*. (A) Implementation procedure of the in situ tumor formation experiment of U251 glioma cells in nude mice. (B) Left, the size and growth status of intracranial tumors were detected 2 h after intramural injection of DMSO (50 mg/kg) or MS170 (50 mg/kg) in nude mice implanted with glioma cells on day 28; three mice in each group are displayed. Right, top, the bioluminescence signals were quantified and analyzed statistically, and bottom, survival curve drawn according to the growth state of nude mice. (C) The glioma tissue of nude mice was stained with hematoxylin and eosin (HE) to show the tumor location and development. The high magnification field of view on the right was the enlarged image of the area marked by the black square frame in the picture on the left. (D) Immunohistochemical staining of glioma tissue in nude mice shows the Ki67 level in the tumor tissue. The high magnification field of view on the right of each group of images was enlarged to the area marked by the black square frame on the left. Scale bars = 100 μm.

indicate the binding efficiency of PROTAC combined with E3 ligase and the target protein, in addition to the degradation efficiency of the target protein. Furthermore, the mutant APR can reflect the binding efficiency of the PROTAC through the bioluminescence curve of luminescence intensity change, but is unable to show the degradation efficiency of the target protein. Currently, there are few PROTACs available for glioma treatment, and their development is challenging, with the BBB being a major obstacle.[22] Overexpression or abnormal activation of AKT is common in glioma; therefore, we mainly explored the value of an APR in glioma.[27] In our study, nude mice were used to establish an orthotopic glioma model (based on stable expression of APR in U251 cells) at 4 weeks of age. Mice were divided into six groups: LALC + DMSO, mLALC + DMSO, LALC + MS170, mLALC + MS170, Luc + DMSO, and Luc + MS170. Mice were injected with MS170 or DMSO intrathecally after tumor implantation every 4 days for 28 days. The mice were closely monitored for their growth status during the culture period (Figure 5A). MS170 had a significant therapeutic effect on glioma, as shown by a significantly lower bioluminescent signal in the Luc + MS170 group compared to the Luc + DMSO group, in addition to better growth status in general (Figure 5B). Both LALC and mLALC showed significant bioluminescence signals compared with corresponding control group, and the mLALC + MS170 group was significantly higher than the LALC + MS170 group (Figure 5B). HE staining and immunohistochemical results also showed that MS170 had a considerable effect, while there was no significant difference in the Ki67 content in tumor tissues of mice in the mLALC + DMSO and mLALC+MS170 groups, which also indicated that mLALC was unable to harvest the therapeutic effect provided by MS170 (Figure 5C,5D). In addition, the protein levels of AKT1 and LA in the glioma tissues of mice in the LALC + MS170 group were significantly lower than those in the mLALC + MS170 group (Figure S5D). The mLALC, as a more advantageous APR, had a significantly different performance compared to LALC due to mutations in CRBN that prevented MS170 from effectively inducing HA-LA degradation and reducing AKT levels. Meanwhile, its excellent reporting performance can be used to screen PROTAC binding efficiency, which is an advantage over LALC. Additionally, we found that the therapeutic effect on tumors could also be feedback through the APR system because APR can show the approximate location and progression of tumors *in vivo* using a live imaging system. In our study, although mLALC did not significantly reduce AKT protein levels, it showed strong bioluminescent signals that were opposite to those observed after MS170 treatment of LALC, indicating that our APR could also be successfully applied *in vivo*.

In summary, we designed an APR that could be effectively applied both *in vitro* and *in vivo* to display the status and

https://doi.org/10.1021/acsomega.4c08186
ACS Omega 2024, 9, 49739−49748

content of the ternary complex (E3-PROTAC-POI) formed with the help of fluorescence or bioluminescent signals. The APR enabled the visualization of the specific binding of the PROTAC within cells, monitoring its ability to induce target protein degradation, as well as its effectiveness in tumor treatment. This tool will greatly assist in the screening of PROTACs and potentially accelerate their development in cancer treatment.

4. DISCUSSION

PROTAC, a mature drug development strategy based on UPS, has received increasing attention. Hundreds of PROTACs have been designed and validated, and the number is still rapidly growing.[10] Despite their considerable advantages and potential applications, and the fact that numerous PROTACs can often be designed for a single target protein, the classical screening process for validating PROTACs is time-consuming and laborious. Although artificial intelligence and machine learning can be used to predict and score PROTACs in the early stages, considerable validation work is still required to select a few highly promising PROTACs. Therefore, the development of a reporter system that can directly display the ternary complex formed between PROTAC, E3, and the target protein is crucial and could accelerate the development of PROTACs.

BiFC analysis is based on the interaction of two proteins to bring their respective coupled nonfluorescent fragments close to each other, thus producing fluorescence signals that can be measured.[16] This technique can simply and directly visualize PPIs in living cells without requiring complex instrumentation, data processing, or exogenous fluorescent dyes.[16] BiFC allows for the dynamic observation of specific protein expression levels and subcellular localization changes, providing more reliable data.[37−39] The multiple fluorescent proteins available for BiFC allows for the simultaneous detection of multiple protein interactions within the same cell, even *in vivo*.[40] However, there are also some limitations of BiFC that should be noted.[16] First, only a few peptide bonds in fluorescent proteins can be disrupted to generate nonfluorescent fragments that bind to form functional complexes, limiting some BiFC-based protein interaction studies. Additionally, there can be a delay between the interaction of fusion proteins and the production of fluorescence due to the slow chemical reactions required for fluorescence complex formation. Despite these limitations, the remarkable performance of the BiFC technique still indicates its significant application prospects and transformation potential.

In our study, we designed and validated a tool for reporting PROTAC performance both *in vitro* and *in vivo*, an APR, which includes essential elements of BiFC, including two nonfluorescent complementary fragments, each fused to the N- or C-terminus of E3 ligase or the POI. Unlike regular BiFC studies that investigate the interaction between E3 ligase and the POI fused with nonfluorescent complementary fragments, our system aimed to investigate the degradation efficiency and binding performance of a PROTAC that can strongly bind to both E3 ligase and the POI. Therefore, APR may display weak fluorescence in the absence of PROTAC on its own, but in the presence of PROTACs, the strong approximation of the two proteins causes the nonfluorescent complementary fragments to approach each other and generate fluorescence, resulting in significantly stronger fluorescence than without PROTACs. Of course, the fluorescence intensity depends on the type of PROTAC and the APR concentration. In addition, we found that when mutating the E2 recruitment site on E3 ligase in the APR without affecting its ability to bind to the PROTAC, the ternary complex can be stably maintained at a high level for a long time in the presence of MS170, thus generating a stable fluorescence signal. We also observed time-dependent characteristics of APR; wild-type E3 ligase causes fluorescence levels to rise steeply at first and then gradually decline under the same conditions, whereas mutated E3 ligase causes fluorescence levels to rise steeply to a maximum point and then remain relatively stable or slightly decline. This maximum point is significantly higher than that of the APR composed of wild-type E3 ligase, indicating that the APR with mutated E3 has advantages as a reporter.

The APR designed in the present study has the following characteristics: (1) The selected fluorescent protein exhibits excellent performance regarding the direct visualization and evaluation of PROTAC drug efficacy. (2) The APR with mutated E3 ligase has strong stability and can avoid proteasomal degradation after binding with the PROTAC. (3) It can be applied both *in vitro* and *in vivo*, with great modification potential for screening and validating PROTACs targeting different proteins. More importantly, we hope that it can serve as a reporting system for screening PROTACs that can cross the BBB, which is also our future research direction. However, there are also limitations to APR that require further validation with larger data sets to improve its applicability. The overexpression of APR may inevitably affect tumor cell development and, thus, affect the screening and validation results. These are areas we need to improve and overcome.

In summary, we designed an effective reporting tool to assess PROTAC performance, the APR, which has great application potential in PROTAC validation both *in vivo* and *in vitro*. This tool is expected to accelerate the drug development and validation process of PROTACs.

■ ASSOCIATED CONTENT

Data Availability Statement

The original contributions presented in the study are included in the article; further inquiries can be directed to the corresponding authors.

Supporting Information

The Supporting Information is available free of charge at https://pubs.acs.org/doi/10.1021/acsomega.4c08186.

Figure S1: EAEC can effectively report the efficacy of PROTAC targeting AKT1; Figure S2: EAEC has significantly higher reporting performance; Figure S3: Reporter properties of EAEC are regulated by MG132, POI ligands or E3 ligands; Figure S4: Specific mutations in E3 can enhance the stability and strength of APR reporting; Figure S5: Time-dependent properties of APR and its reporting effects *in vivo* (PDF)

■ AUTHOR INFORMATION

Corresponding Authors

Xingen Zhu − *Department of Neurosurgery, The Second Affiliated Hospital, Jiangxi Medical College, Nanchang University, Nanchang, Jiangxi 330006, P. R. China; Institute of Neuroscience, Nanchang University, Nanchang, Jiangxi 330006, P. R. China*; Email: ndefy89006@ncu.edu.cn

Kai Huang − *Department of Neurosurgery, The Second Affiliated Hospital, Jiangxi Medical College, Nanchang University, Nanchang, Jiangxi 330006, P. R. China; Institute*

https://doi.org/10.1021/acsomega.4c08186
ACS Omega 2024, 9, 49739−49748

of Neuroscience, Nanchang University, Nanchang, Jiangxi 330006, P. R. China; Email: kaihuang@ncu.edu.cn

Authors

Kunjian Lei − *Department of Neurosurgery, The Second Affiliated Hospital, Jiangxi Medical College, Nanchang University, Nanchang, Jiangxi 330006, P. R. China; Institute of Neuroscience, Nanchang University, Nanchang, Jiangxi 330006, P. R. China*

Yilei Sheng − *Department of Neurosurgery, The Second Affiliated Hospital, Jiangxi Medical College, Nanchang University, Nanchang, Jiangxi 330006, P. R. China; Institute of Neuroscience, Nanchang University, Nanchang, Jiangxi 330006, P. R. China*

Yishuang Li − *Department of Neurosurgery, The Second Affiliated Hospital, Jiangxi Medical College, Nanchang University, Nanchang, Jiangxi 330006, P. R. China; Institute of Neuroscience, Nanchang University, Nanchang, Jiangxi 330006, P. R. China*

Zhihong Zhou − *Department of Neurosurgery, The Second Affiliated Hospital, Jiangxi Medical College, Nanchang University, Nanchang, Jiangxi 330006, P. R. China; Institute of Neuroscience, Nanchang University, Nanchang, Jiangxi 330006, P. R. China*

Complete contact information is available at: https://pubs.acs.org/10.1021/acsomega.4c08186

Author Contributions

X.Z. and K.H. were the designer of this study, The main experimental work was completed by K.L. Y.L. jointly completed the construction of the plasmid, and Z.Z. provided help in vivo experiments, The manuscript was written by K.L. All authors discussed the results and commented on the manuscript.

Notes

The authors declare no competing financial interest.

All in vivo experimental procedures were ethically compliant and approved by the Institutional Animal Care and Use Committee of Nanchang University.

■ ACKNOWLEDGMENTS

This research was funded by the National Natural Science Foundation (grant nos. 82002660, 82172989, and 81960456), Key Research and Development Program of Jiangxi Province (grant no. 20212BBG73021), Major Discipline Academic and Technical Leaders Training Program of Jiangxi Province -- Young talents program (grant no. 20212BCJ23023), Key Science and Technology Research Project in Jiangxi Province Department of Education (grant no. GJJ210177), and College Students' Innovative Entrepreneurial Training Plan Program (no. 202210403026).

■ REFERENCES

(1) Zhao, L.; Zhao, J.; Zhong, K.; Tong, A.; Jia, D. Targeted protein degradation: mechanisms, strategies and application. *Signal Transduction Targeted Ther.* **2022**, *7*, No. 113.

(2) Luh, L. M.; Scheib, U.; Juenemann, K.; et al. Prey for the Proteasome: Targeted Protein Degradation-A Medicinal Chemist's Perspective. *Angew. Chem., Int. Ed.* **2020**, *59*, 15448−15466.

(3) Schapira, M.; Calabrese, M. F.; Bullock, A. N.; Crews, C. M. Targeted protein degradation: expanding the toolbox. *Nat. Rev. Drug Discovery* **2019**, *18*, 949−963.

(4) de Duve, C. The lysosome turns fifty. *Nat. Cell Biol.* **2005**, *7*, 847−849.

(5) Dikic, I. Proteasomal and Autophagic Degradation Systems. *Annu. Rev. Biochem.* **2017**, *86*, 193−224.

(6) Eldridge, A. G.; O'Brien, T. Therapeutic strategies within the ubiquitin proteasome system. *Cell Death Differ.* **2010**, *17*, 4−13.

(7) Yuan, T.; Yan, F.; Ying, M.; et al. Inhibition of Ubiquitin-Specific Proteases as a Novel Anticancer Therapeutic Strategy. *Front. Pharmacol.* **2018**, *9*, 1080.

(8) Deng, L.; Meng, T.; Chen, L.; Wei, W.; Wang, P. The role of ubiquitination in tumorigenesis and targeted drug discovery. *Signal Transduction Targeted Ther.* **2020**, *5*, No. 11.

(9) Chen, Y.; Tandon, I.; Heelan, W.; et al. Proteolysis-targeting chimera (PROTAC) delivery system: advancing protein degraders towards clinical translation. *Chem. Soc. Rev.* **2022**, *51*, 5330−5350.

(10) Békés, M.; Langley, D. R.; Crews, C. M. PROTAC targeted protein degraders: the past is prologue. *Nat. Rev. Drug Discov* **2022**, *21*, 181−200.

(11) Faux, M. C.; Scott, J. D. Molecular glue: kinase anchoring and scaffold proteins. *Cell* **1996**, *85*, 9−12.

(12) Dong, G.; Ding, Y.; He, S.; Sheng, C. Molecular Glues for Targeted Protein Degradation: From Serendipity to Rational Discovery. *J. Med. Chem.* **2021**, *64*, 10606−10620.

(13) Burslem, G. M.; Crews, C. M. Proteolysis-Targeting Chimeras as Therapeutics and Tools for Biological Discovery. *Cell* **2020**, *181*, 102−114.

(14) Zeng, S.; Huang, W.; Zheng, X.; et al. Proteolysis targeting chimera (PROTAC) in drug discovery paradigm: Recent progress and future challenges. *Eur. J. Med. Chem.* **2021**, *210*, No. 112981.

(15) Bushweller, J. H. Targeting transcription factors in cancer - from undruggable to reality. *Nat. Rev. Cancer* **2019**, *19*, 611−624.

(16) Kerppola, T. K. Bimolecular fluorescence complementation (BiFC) analysis as a probe of protein interactions in living cells. *Annu. Rev. Biophys* **2008**, *37*, 465−487.

(17) Cevheroğlu, O.; Kumas, G.; Hauser, M.; Becker, J. M.; Son, C. D. The yeast Ste2p G protein-coupled receptor dimerizes on the cell plasma membrane. *Biochim. Biophys. Acta, Biomembr.* **2017**, *1859*, 698−711.

(18) Pathmanathan, S.; Barnard, E.; Timson, D. J. Interactions between the budding yeast IQGAP homologue Iqg1p and its targets revealed by a split-EGFP bimolecular fluorescence complementation assay. *Cell Biol. Int.* **2008**, *32*, 1318−1322.

(19) Paulmurugan, R.; Umezawa, Y.; Gambhir, S. S. Noninvasive imaging of protein-protein interactions in living subjects by using reporter protein complementation and reconstitution strategies. *Proc. Natl. Acad. Sci. U. S. A.* **2002**, *99*, 15608−15613.

(20) Ozawa, T.; Takeuchi, T. M.; Kaihara, A.; Sato, M.; Umezawa, Y. Protein splicing-based reconstitution of split green fluorescent protein for monitoring protein-protein interactions in bacteria: improved sensitivity and reduced screening time. *Anal. Chem.* **2001**, *73*, 5866−5874.

(21) Ozawa, T.; Kaihara, A.; Sato, M.; Tachihara, K.; Umezawa, Y. Split luciferase as an optical probe for detecting protein-protein interactions in mammalian cells based on protein splicing. *Anal. Chem.* **2001**, *73*, 2516−2521.

(22) van Tellingen, O.; Yetkin-Arik, B.; de Gooijer, M.; et al. Overcoming the blood-brain tumor barrier for effective glioblastoma treatment. *Drug Resistance Updates* **2015**, *19*, 1−12.

(23) Han, L.; Jiang, C. Evolution of blood-brain barrier in brain diseases and related systemic nanoscale brain-targeting drug delivery strategies. *Acta Pharm. Sin. B* **2021**, *11*, 2306−2325.

(24) Lei, K.; Li, J.; Tu, Z.; et al. Prognostic and Predictive Value of Immune-Related Gene Pair Signature in Primary Lower-Grade Glioma Patients. *Front. Oncol.* **2021**, *11*, No. 665870.

(25) Li, X.; Song, Y. Proteolysis-targeting chimera (PROTAC) for targeted protein degradation and cancer therapy. *J. Hematol. Oncol.* **2020**, *13*, No. 50.

(26) Wakabayashi, Y.; Nariya, H.; Yasugi, M.; et al. An enhanced green fluorescence protein (EGFP)-based reporter assay for

quantitative detection of sporulation in *Clostridium perfringens* SM101. *Int. J. Food Microbiol.* **2019**, *291*, 144−150.
(27) Chautard, E.; Ouedraogo, Z. G.; Biau, J.; Verrelle, P. Role of Akt in human malignant glioma: from oncogenesis to tumor aggressiveness. *J. Neurooncol* **2014**, *117*, 205−215.
(28) Brennan, C. W.; Verhaak, R.; McKenna, A.; et al. The somatic genomic landscape of glioblastoma. *Cell* **2013**, *155*, 462−477.
(29) You, I.; Erickson, E. C.; Donovan, K. A.; et al. Discovery of an AKT Degrader with Prolonged Inhibition of Downstream Signaling. *Cell Chem. Biol.* **2020**, *27*, 66−73 e67.
(30) Yu, X.; Xu, J.; Shen, Y.; et al. Discovery of Potent, Selective, and In Vivo Efficacious AKT Kinase Protein Degraders via Structure-Activity Relationship Studies. *J. Med. Chem.* **2022**, *65*, 3644−3666.
(31) Yu, X.; Xu, J.; Xie, L.; et al. Design, Synthesis, and Evaluation of Potent, Selective, and Bioavailable AKT Kinase Degraders. *J. Med. Chem.* **2021**, *64*, 18054−18081.
(32) Belair, D. G.; Lu, G.; Waller, L. E.; et al. Thalidomide Inhibits Human iPSC Mesendoderm Differentiation by Modulating CRBN-dependent Degradation of SALL4. *Sci. Rep.* **2020**, *10*, No. 2864.
(33) Matyskiela, M. E.; Lu, G.; Ito, T.; et al. A novel cereblon modulator recruits GSPT1 to the CRL4(CRBN) ubiquitin ligase. *Nature* **2016**, *535*, 252−257.
(34) Williams, S. J.; Prescher, J. A. Building Biological Flashlights: Orthogonal Luciferases and Luciferins for in Vivo Imaging. *Acc. Chem. Res.* **2019**, *52*, 3039−3050.
(35) Prescher, J. A.; Contag, C. H. Guided by the light: visualizing biomolecular processes in living animals with bioluminescence. *Curr. Opin. Chem. Biol.* **2010**, *14*, 80−89.
(36) Chen, H.; Zou, Y.; Shang, Y.; et al. Firefly luciferase complementation imaging assay for protein-protein interactions in plants. *Plant Physiol.* **2008**, *146*, 368−376.
(37) Fang, D.; Kerppola, T. K. Ubiquitin-mediated fluorescence complementation reveals that Jun ubiquitinated by Itch/AIP4 is localized to lysosomes. *Proc. Natl. Acad. Sci. U. S. A.* **2004**, *101*, 14782−14787.
(38) Guo, H. X.; Cun, W.; Liu, L. D.; et al. Protein encoded by HSV-1 stimulation-related gene 1 (HSRG1) interacts with and inhibits SV40 large T antigen. *Cell Proliferation* **2006**, *39*, 507−518.
(39) Fan, M.; Ahmed, K. M.; Coleman, M. C.; Spitz, D. R.; Li, J. J. Nuclear factor-kappaB and manganese superoxide dismutase mediate adaptive radioresistance in low-dose irradiated mouse skin epithelial cells. *Cancer Res.* **2007**, *67*, 3220−3228.
(40) Hu, C. D.; Kerppola, T. K. Simultaneous visualization of multiple protein interactions in living cells using multicolor fluorescence complementation analysis. *Nat. Biotechnol.* **2003**, *21*, 539−545.

https://doi.org/10.1021/acsomega.4c08186
ACS Omega 2024, 9, 49739−49748